

# SUMER-Hinode observations of microflares: excitation of molecular hydrogen

D. E. Innes

Max-Planck Institut für Sonnensystemforschung, 37191 Katlenburg-Lindau, Germany  
e-mail: innes@mps.mpg.de

Received —; accepted —

## ABSTRACT

**Context.** Concentrations of  $H_2$  have been detected by SUMER in active region plage. The  $H_2$  is excited by  $O\text{ VI}$  line emission at 1031.94 Å which, although not observed, must be brightening along with the observed transition region line,  $Si\text{ III}$  1113.24 Å.

**Aims.** We investigate the excitation of  $H_2$  and demonstrate the association between the observed  $H_2$  emission and footpoints of X-ray microflares.

**Methods.** We have made co-ordinated observations of active region plage with the spectrometer SUMER/SoHO in lines of  $H_2$  1119.10 Å and  $Si\text{ III}$  1113.24 Å and with XRT/Hinode X-ray and SOT/Hinode  $Ca\text{ II}$  filters.

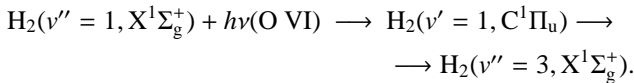
**Results.** In six hours of observation, six of the seven  $H_2$  events seen occurred near a footpoint of a brightening X-ray loop. The seventh is associated with an unusually strong  $Si\text{ III}$  plasma outflow.

**Conclusions.** Microflare energy dissipation heats the chromosphere, reducing its opacity, so that  $O\text{ VI}$  microflare emission is able to reach the lower layers of the chromosphere and excite the  $H_2$ .

**Key words.** molecular processes – Sun: activity – Sun: flares – Sun: UV radiation

## 1. Introduction

Solar  $H_2$  emission is strong in ultraviolet spectra of sunspots and has also been seen in flares (Bartoe et al. 1979). In the quiet Sun it is present but extremely weak (Sandlin et al. 1986). Here we report the first observations of  $H_2$  concentrations in bright active region plage. The observed  $H_2$  line at 1119.10 Å is the 1–3 transition in the Werner series, excited by  $O\text{ VI}$  1032 Å (Bartoe et al. 1979; Schühle et al. 1999):



The 1119.10 Å line is about 60 % as bright as the strongest 1–4 Werner line at 1164 Å. The  $H_2$  is believed to be formed just above the temperature minimum at around 4200 K. Its strength is expected to correlate with the  $O\text{ VI}$  intensity, as well as with the chromosphere structure in and above the  $H_2$  region (Jordan et al. 1978).

In this letter, three types of  $H_2$  plage events are discussed. The strongest coincided with ribbon-like  $Ca\text{ II}$  chromospheric brightening at a footpoint of an X-ray microflare. The second occurred near the footpoint of a brightening X-ray loop with no signature in  $Ca\text{ II}$ , and the third had neither X-ray emission nor a  $Ca\text{ II}$  signature but very strong transition region outflow. All three events highlighted here occurred in three hours on one of the observing days. During the second day of observation, three  $H_2$  events were detected in three hours, and all were associated with X-ray loop brightening with no  $Ca\text{ II}$  signature.

## 2. Observations

Hinode (Kosugi et al. 2007) and SUMER (Wilhelm et al. 1995) observed a small active region (AR 10953) on 29 and 30 Apr 2007. The region had produced several B and one C class flare four days earlier. All events during the observing period discussed here were below B class. On each day, SUMER made six rasters across the plage and sunspot. Each raster took 30 min. The lines observed were  $H_2$  1119.10 Å ( $4.2 \times 10^3$  K),  $C\text{ I}$  multiplet at 1114.39 Å and 1118.41 Å ( $10^4$  K),  $Si\text{ III}$  1113.24 Å ( $6 \times 10^4$  K), and  $Ca\text{ II}$  8500 Å ( $7 \times 10^5$  K), where the approximate formation temperatures of the lines are given in brackets. The spectrum across the sunspot is shown in Fig. 1. The sunspot is seen predominantly in the  $H_2$  line.

Hinode made simultaneous observations with the X-Ray Telescope (XRT; Golub et al. 2007) through both the Ti-poly and Al-thick filters with 1.5 min cadence. Observations through both the  $Ca\text{ II}$  and G-band filters were made with the Broadband Filter Imager of the Solar Optical Telescope (SOT; Tsuneta et al. 2007) with a 1 min cadence. The Extreme ultraviolet Imaging Spectrometer (EIS; Culhane et al. 2007) observed  $Fe\text{ xv}$  284.25 Å ( $2 \times 10^6$  K), using the wide 266'' slit and 15 s cadence. To obtain the coalignment between the X-ray images and SUMER, the EIS images were very useful because they bridged the gap between SOT  $Ca\text{ II}$  and XRT. In particular, during the strongest microflare event, EIS captured both the X-ray loop seen with XRT and the ribbon-like footpoint structure seen in the SOT  $Ca\text{ II}$  images. This provided the SOT, XRT, and EIS coalignment. The SUMER-SOT coalignment was made by comparing SOT G-band and SUMER  $H_2$  images. Additional checks were done by comparing SUMER  $Si\text{ III}$  and EIS  $Fe\text{ xv}$ . The coalignment between SUMER and XRT is believed to be better than 5'', with greater accuracy in the north-south (sun-y) direction.

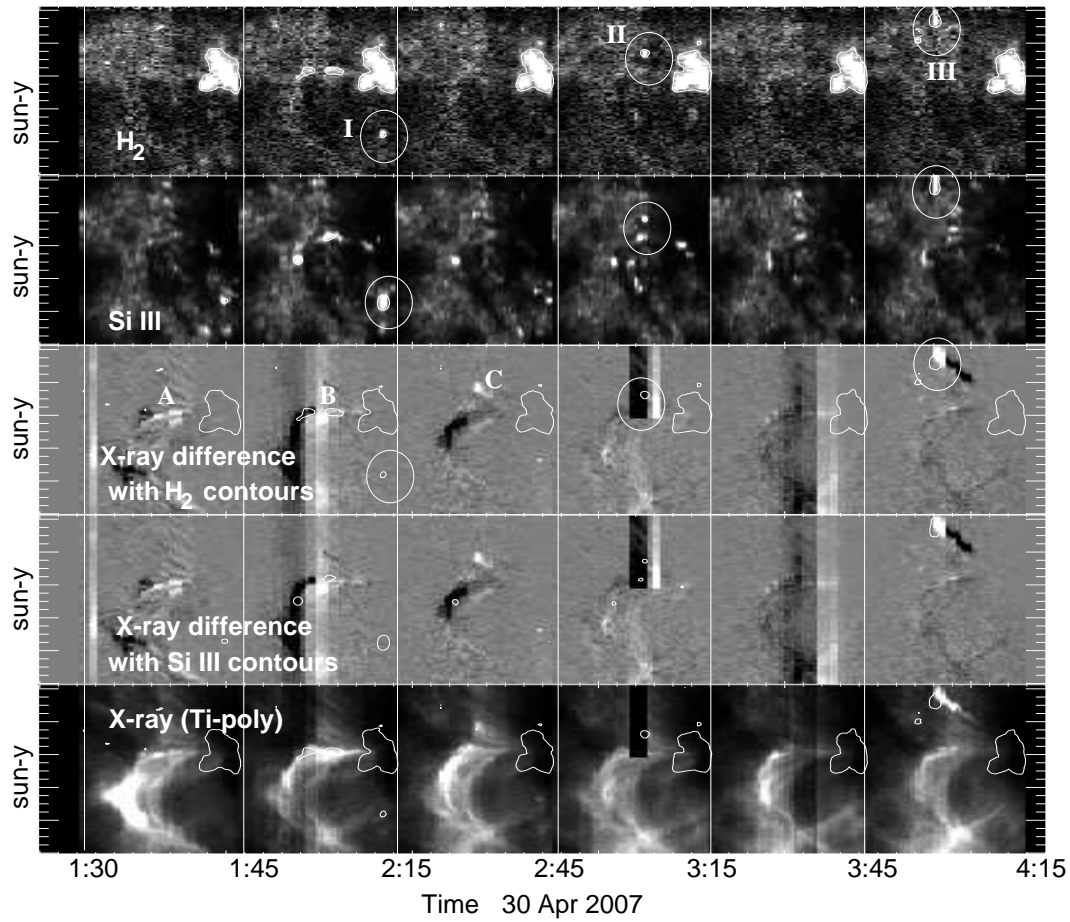


**Fig. 2.** The six raster scans taken in H<sub>2</sub> and Si III, and the equivalent X-ray time-slice rasters. The X-ray rasters are constructed by stacking, for each SUMER observation, the cospatial XRT slices from the XRT Ti-poly images closest in time. The difference images are computed by subtracting the preceding XRT Ti-poly image. The plage H<sub>2</sub> brightenings (labelled I, II, III) are circled in the H<sub>2</sub>, Si III, and top X-ray difference raster. The H<sub>2</sub> contours are at  $8 \times 10^{-3}$  photons s<sup>-1</sup> m<sup>-2</sup> sr<sup>-1</sup>, and Si III contours are at 1.2 photons s<sup>-1</sup> m<sup>-2</sup> sr<sup>-1</sup>. All images have a linear intensity scale. The sun-x and sun-y co-ordinates are as in Fig. 3

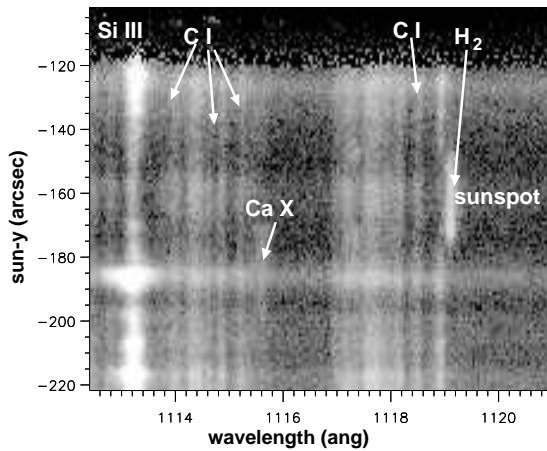


**Fig. 1.** SUMER spectrum of the region across and around the sunspot, taken on 29 Apr 2007 at 02:25 UT.

The six rasters taken on 30 Apr 2007 are shown as a time series in Fig. 2. Here, the sunspot is the bright H<sub>2</sub> region on the right of each raster. The linear intensity scale used to display the images accentuates the few plage brightenings, both in the H<sub>2</sub>

and the Si III images. The three brightest H<sub>2</sub> concentrations are circled and labelled I, II, III. Each H<sub>2</sub> concentration coincides with intense Si III, but the inverse is not true. Not all Si III brightenings are associated with H<sub>2</sub>. The relationship between the H<sub>2</sub> and X-ray brightenings is shown in the third row of Fig. 2. The two strongest H<sub>2</sub> events, II and III, are associated with X-ray brightenings. Unfortunately, the X-ray brightening at II is exaggerated by a data gap. Its brightening is seen better in the XRT difference images displayed in Fig. 3. Event III was much the brightest X-ray event during the observing period. This is the event, mentioned previously, that coincided with a small, bright ribbon-like structure seen in Ca II images. Close inspection of the X-ray difference rasters reveals additional X-ray brightenings, labelled A, B, and C in the third row of Fig. 2. Event B is associated with weak H<sub>2</sub> and Si III, and A and C only with weak Si III.

The SUMER spectra of the circled events (I, II, and III) are shown in Fig. 4. There is no simple relationship between the Si III strength and the H<sub>2</sub>. In each case the H<sub>2</sub> strength is 1 – 1.5 DN, whereas the Si III varies by a factor of three. It is noticeable that the Si III emission is generally broader. In event II, it is offset by 2'' from the H<sub>2</sub>.

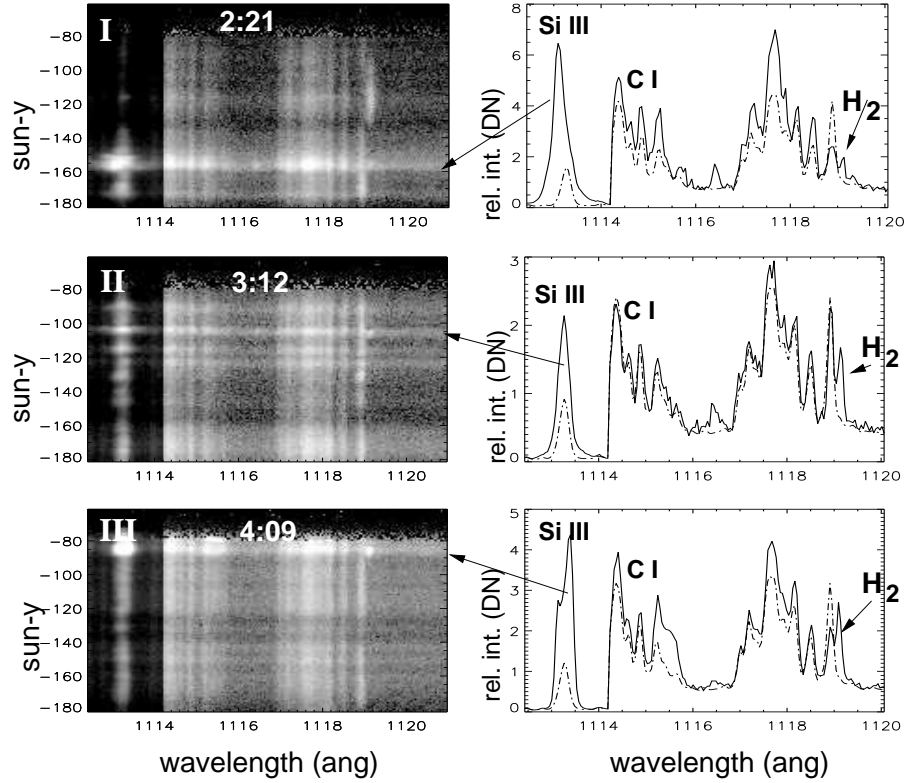


**Fig. 4.** SUMER spectral images and profiles of the H<sub>2</sub> brightenings. The Si III intensity is reduced by a factor 20 compared to the rest of the spectrum, so that they can be displayed with the same scale. Each H<sub>2</sub> spectrum is compared to the average plate spectrum, which has been scaled so that their continua at 1116 Å match.

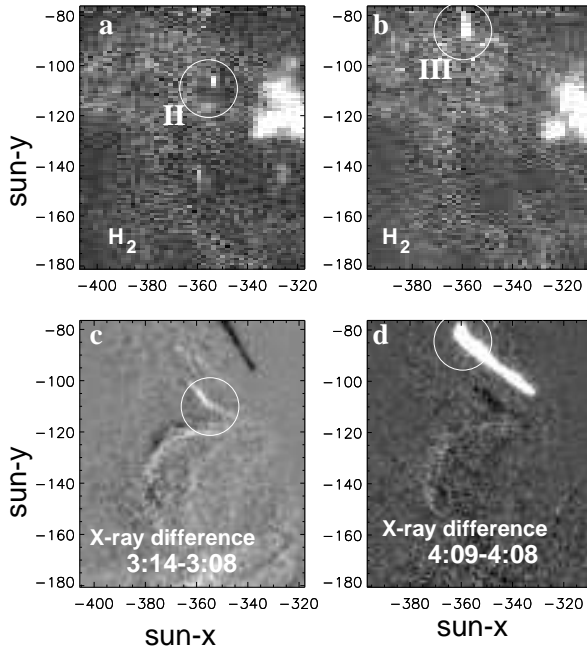


**Fig. 3.** SUMER raster images of H<sub>2</sub> (top row) and, below, the XRT Ti-poly difference images at the time of the H<sub>2</sub> brightenings.

### 3. Discussion

The H<sub>2</sub> intensity depends on both the strength of the O VI and the atmospheric opacity between the O VI and H<sub>2</sub> layers. If the O VI

follows the Si III brightness, then an increase in transition region emission cannot be the only reason for enhanced H<sub>2</sub> excitation, because there are several examples of bright Si III and no observed H<sub>2</sub>. The analyses by Jordan et al. (1978) and Bartoe et al. (1979) of H<sub>2</sub> in a sunspot and quiet Sun led them to conclude that the opacity over the sunspot is about an order of magnitude less than in the quiet Sun. This suggests a similar explanation for the H<sub>2</sub> concentrations in bright plage because energy dissipation at X-ray loop footpoints is commonly associated with chromospheric evaporation, and the two strongest events discussed here and all three events seen on 29 April 2007 were associated with X-ray loop brightening. The one event not associated with X-ray brightening showed significant plasma outflow from the transition region.

If chromospheric evaporation due to high-energy particles accelerated in the microflare reduces the opacity of the chromosphere, one might expect to find a relationship between the X-ray emission and the H<sub>2</sub>. This is not confirmed by the observations presented here, but this could be because the observed H<sub>2</sub> strength depends critically on the position of the loop footpoint in relation to the SUMER field-of-view at the time of the brightening. The reason more Si III and X-ray coincidences occur is probably because Si III brightenings come from higher up in the atmosphere and cover a larger area, and not just from the loop footpoint.

Future observations with SUMER will measure the O VI 1032 Å and H<sub>2</sub> intensities almost simultaneously. This, together with extended SOT observations and analysis of the chromospheric dynamics, will help determine the extent and influence of opacity changes on the H<sub>2</sub> intensity.

*Acknowledgements.* I would like to thank Maria Madjarska for her constructive comments and careful reading of this letter. Hinode is a Japanese mission developed and launched by ISAS/JAXA, collaborating with NAOJ, as domestic partner, and NASA (USA) and STFC (UK) as international partners. Scientific operation of the Hinode mission is conducted by the Hinode science team organized at ISAS/JAXA. Support for the postlaunch operation is provided by JAXA and NAOJ, STFC, NASA, ESA (European Space Agency), and NSC (Norway). SUMER is financially supported by DLR, CNES, NASA, and the ESA PRODEX program (Swiss contribution). SoHO is a project of international co-operation between ESA and NASA. We are grateful to all teams for their efforts in the design, building, and operation of the Hinode and SoHO missions.

## References

- Bartoe, J.-D. F., Brueckner, G. E., Nicolas, K. R., et al. 1979, MNRAS, 187, 463  
 Culhane, J. L., Harra, L. K., James, A. M., et al. 2007, Sol. Phys., 60  
 Golub, L., Deluca, E., Austin, G., et al. 2007, Sol. Phys., 243, 63  
 Jordan, C., Brueckner, G. E., Bartoe, J.-D. F., Sandlin, G. D., & Vanhoosier, M. E. 1978, ApJ, 226, 687  
 Kosugi, T., Matsuzaki, K., Sakao, T., et al. 2007, Sol. Phys., 118  
 Sandlin, G. D., Bartoe, J.-D. F., Brueckner, G. E., Tousey, R., & Vanhoosier, M. E. 1986, ApJS, 61, 801  
 Schühle, U., Brown, C. M., Curdt, W., & Feldman, U. 1999, in ESA Special Publication, Vol. 446, 8th SOHO Workshop: Plasma Dynamics and Diagnostics in the Solar Transition Region and Corona, ed. J.-C. Vial & B. Kaldeich-Schü, 617  
 Tsuneta, S., Ichimoto, K., Katsukawa, Y., et al. 2007, ArXiv e-prints, 711.1715  
 Wilhelm, K., Curdt, W., Marsch, E., et al. 1995, Sol. Phys., 162, 189